Javier GALLARDO-LOZANO, Maria Isabel MILANÉS-MONTERO, Miguel Angel GUERRERO-MARTÍNEZ, Enrique ROMERO-CADAVAL

School of Industrial Engineering. University of Extremadura

Non-disturbing bidirectional charger for PHEVs and EVs

Abstract. *A new algorithm for a bidirectional battery charger for PHEVs (Plug-in Electric Vehicles) and EVs (Electric Vehicles) is proposed. It achieves the battery charging and the Vehicle-to-Grid (V2G) modes, demanding or injecting currents into the grid without harmonics and with unity displacement power factor, regardless of whether the grid voltage is ideal (sinusoidal) or distorted, as the generated reference current is obtained from the fundamental component of the phase-neutral grid voltage, contributing to the concept of Smart Grids. Simulation and experimental results are included to validate the design (topology and its control) of the proposed charger.*

Streszczenie. *Zaproponowano nowy algorytm dwukierunkowego układu ładowania baterii dla pojazdów elektrycznych. System zapewnia ładowanie baterii bez wprowadzania zakłóceń do sieci. (**Nowy dwukierunkowy system ładowania baterii do samochodów elektrycznych**)*

Keywords: Bidirectional charger, battery, EV, V2G, non-disturbance, smart grids.
Słowa kluczowe: ładowanie baterii, pojazdy elektryczne..

Introduction

The fossil fuel has been the dominant primary source of energy in the existing transport. However, it is common knowledge that the reserves of fuel in the Earth are limited. In addition, due to the instability in Middle East and the increasing concern for the ecosystem, alternative energy is acquiring major relevance.

Nowadays, the research on more efficient vehicles has motivated the development of Plug-in Hybrid Electric Vehicles (PHEV) and Electric Vehicles (EV). There are commercial EVs in the market, with chargers to connect the vehicle to the grid, but these chargers allow only the charging of the battery, and demand a current with a high distortion. From the grid point of view, these PHEVs and EVs behave as non-linear loads, causing harmonic disturbances in the voltage at the point of coupling. Taking into account the exponential increase in the usage of EVs expected in the next years, it is very essential to develop non-disturbing chargers in order to contribute to improve the power quality of the electrical distribution system.

Along the last years, a great study and development of the battery chargers for PHEVs and EVs has been carried out [1]-[7], but most of them can only charge the battery and others, very similar to the work presented in this paper [8], do not take into account the grid power quality.

Along the following lines, a novel single-phase bidirectional charger is proposed, as it lets a V2G (Vehicle-to-Grid) and a G2V (Grid-to-Vehicle) modes (the energy flows from the vehicle battery to the grid and from the grid to the battery, respectively) and it is carried out taking into account the power quality. The battery charging and discharging are achieved demanding or injecting into the grid currents without harmonics and with unity displacement power factor, regardless of whether the grid voltage is ideal (sinusoidal) or distorted, contributing to the concept of Smart Grids. No disturbances in the grid voltage can affect the generated reference current to demand or inject into the grid, as the reference current is generated from the fundamental component of the phase-neutral grid voltage. In addition, any battery technology can be used.

Simulation and experimental results are included to verify the design of the proposed charger.

Battery Charger Topology

This single-phase bidirectional battery charger allows a battery charging mode (flow from the grid towards the battery, what corresponds to a negative battery current) and a battery discharging mode (flow from the battery towards the grid, what corresponds to a positive battery current). Any technology of battery can be used. It has two power stages, as shown in Fig. 1: stage 1 is a DC/DC bidirectional converter; stage 2 is a single-phase bidirectional inverter.

The DC/DC converter adapts the battery output voltage to the suitable inverter input voltage and fixed it to a constant level regardless of a battery voltage variation due to its State-Of-Charge (SOC). The aim of the bidirectional inverter is whether to convert the DC values (from the DC/DC converter) to the suitable AC values, in order to inject sinusoidal currents in phase with the voltage into the grid, or to convert the AC values (from the grid) to the suitable constant DC values with which the DC/DC converter works.

The bidirectional DC/DC converter, shown in Fig. 2, is explained in [9].

An H-bridge topology is used for the bidirectional inverter, as it is shown in Fig. 3. The mid-point of each leg is connected to the grid by a filter inductor with an internal resistance R_{AC} and an inductance L_{AC}. In order to achieve a proper operation of the inverter, it is necessary to satisfy

$$U_{dc} > \hat{u}_{AN} \tag{1}$$

where: U_{dc} – DC inverter input voltage, $\hat{u}_{AN}$ – peak value of the phase-neutral voltage (which is the maximum instantaneous value it can reach).

The inverter can work in two different configurations:

a) S1-ON; S2-OFF

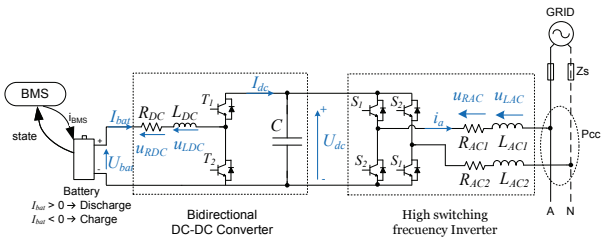

Fig.1. General electric diagram of the bidirectional charger

Analyzing the inverter and neglecting the drop voltage of R_{AC}, it can be obtained

$$u_L = L_{AC}\frac{di_a}{dt} = \frac{U_{dc} - u_{AN}}{2} > 0 \tag{2}$$

where: u_L – inductor voltage, i_a – inverter output current, u_{AN} – instantaneous phase-neutral grid voltage.

u_L is always positive since (1) is assumed and its variation is negligible during the sample time, so it is considered that it remains constant during this period.

It can be concluded that the inverter output current is a straight line with a positive slope

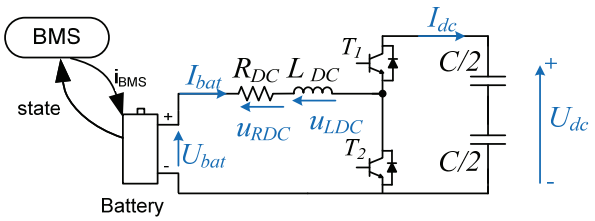

Fig.2. Electric diagram of the DC/DC converter

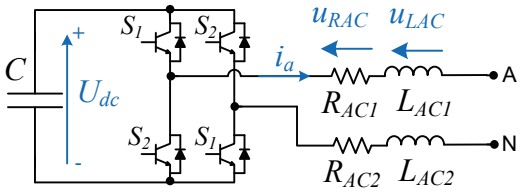

Fig.3. Electric diagram of the three-phase inverter

b) S1-OFF; S2-ON

A new analysis provides

$$u_L = \frac{-U_{dc} - u_{AN}}{2} < 0 \quad (3)$$

According to (1), u_L is always negative and it can be concluded that the inverter output current is a straight line with a negative slope.

Battery

A great variety of battery models has been implemented to be able to simulate the battery behaviour in PHEV and EV [10]-[15]. In this paper, a battery model has been implemented to be able to simulate the behaviour of three types of batteries: Lead-Acid, Nickel-Metal-Hydride (NiMH) and Lithium-Ion (Li-ion). A model based on a controlled voltage source in series with a constant resistance has been used, as it is shown in Fig.4.

The controlled voltage source is modelled with a non-linear equation [16].

The parameters of the model are obtained from the manufacturer's discharge curve and the electrical characteristics from the datasheet of the battery, as shown in Fig.5.

In addition, to complete the battery model and take into account the self-discharge in case the car is parked and left for long time, a new block has been designed and inserted into the battery model to include this parameter.

The self-discharge is measured as the percentage per month of reduced stored charge of the battery without any connection between the electrodes, so the proposed block adds to the input current an additional amount that causes a battery discharge equivalent to the self-discharge and it is implemented as shown in Fig.6.: no connection between the electrodes is detected when the battery current is zero and no variation occurs, what implies that the battery current and its derivative is zero. This detection keeps in memory the value that the SOC had when the disconnection occurred and calculates the amount of current needed to simulate the correct self-discharge.

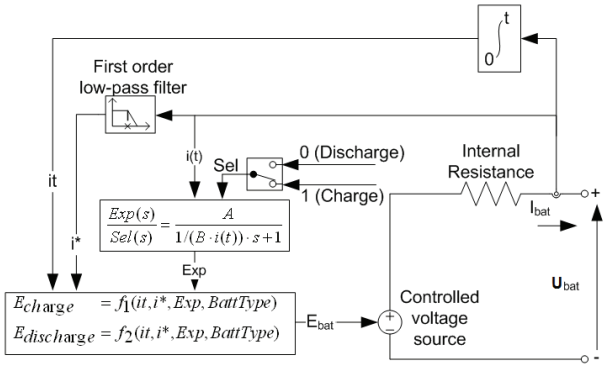

Fig.4. Non-linear battery model

Electrical characteristics	
Nominal voltage (V)	1.2
Typical capacity (mAh)*	11000
IEC minimum capacity (mAh)*	10000
IEC designation	HRMT 33/91
Impedance at 1000 Hz (mΩ)	5

* Charge 16 h at C/10, discharge at C/5.

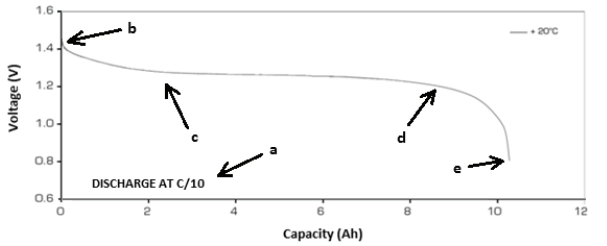

Fig.5. Obtaining of battery model parameters from manufacturer's datasheet of Saft Ni-MH VHT F.

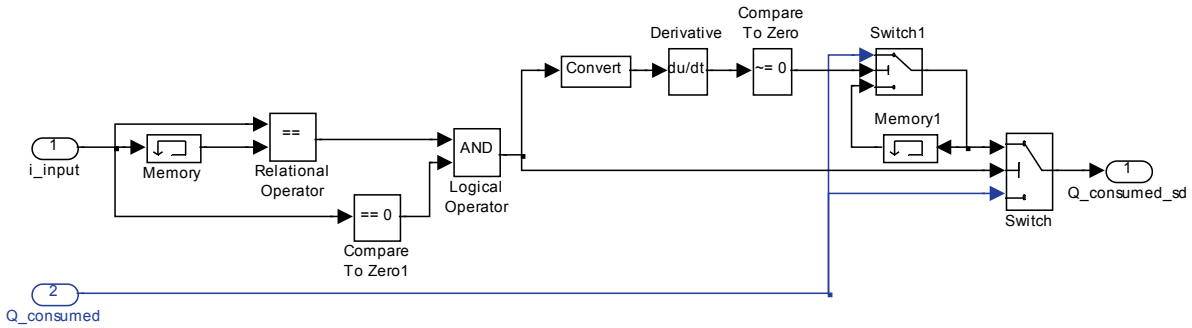

Fig.6. Non-linear battery model

Generation of the converters reference currents

The DC/DC converter is controlled by the battery current, I_{bat}, and its reference current value comes from the Battery Management System (BMS) as follows:

$$I_{bat,ref} = I_{BMS} \tag{4}$$

where: $I_{bat,ref}$ – reference battery current, I_{BMS} – BMS current.

A novel Sinusoidal Source Current control strategy is proposed for the bidirectional inverter. The aim of this control strategy is that the charger injects (or demand) into the grid a current without harmonics, in phase with the fundamental component of the phase-neutral grid voltage, attaining a unity displacement power factor.

The inverter reference current, $\vec{i}_{a,ref}$, is obtained multiplying a constant, K, by the unit vector of the fundamental component of the phase-neutral grid voltage, $\vec{u}_{AN_1}$,

$$\vec{i}_{a,ref} = K \cdot \vec{u}_{AN_1} = I_A \cdot \vec{u}_{AN_1} \tag{5}$$

where: I_A – RMS value of the injected (or demanded) current into the grid.

The output instantaneous power is calculated as

$$p_{AN}(t) = u_{AN} i_a \tag{6}$$

where: $p_{AN}(t)$, u_{AN}, i_a – inverter output power, voltage and current.

Equation (5) is calculated according to

$$i_{a,ref} = \frac{P_{AN}}{U_{AN_1}^2} \cdot \vec{u}_{AN_1} \tag{7}$$

where: P_{AN} - the inverter output active power (calculated as the mean value of $p_{AN}(t)$), U_{AN1} - the RMS fundamental component of the phase-neutral grid voltage.

The unit vector is calculated as

$$\vec{u}_{AN_1} = \frac{u_{AN_1}}{U_{AN_1}} \tag{8}$$

where: u_{AN_1} - the instantaneous fundamental component of the phase-neutral grid voltage.

Neglecting the power losses in the charger, P_{AN} equals the mean value of the charger input power, so equation (7) can be finally solved as

$$i_{a,ref} = \frac{P_{AN}}{U_{AN_1}^2} \cdot u_{AN_1} = \frac{\overline{U_{bat} \cdot I_{bat}}}{U_{AN_1}^2} \cdot u_{AN_1} \tag{9}$$

where: U_{bat}- the battery voltage, I_{bat}- the battery current.

Fig.7 shows the Matlab/Simulink block diagram to generate the inverter reference current. An Autoadjustable Synchronous Reference Frame (ASRF) has been used to obtain the fundamental component of the grid voltage [17].

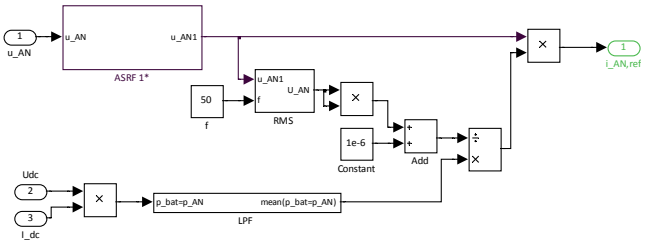

Fig.7. Block diagram of the control strategy of the inverter

Tracking technique

The switching signals of both converters are generated with a synchronous hysteresis band controller. At every sample time, the measured current is compared with the reference current (equation (4) and (9), depending on the converter). In case the measured current is lower than the reference one, a positive slope for the current is needed to decrease the error and the configuration a) is applied, otherwise, configuration b) is carried out (see Fig.8 in case of the DC/DC converter).

Simulation

Fig.9 shows the complete system, performed using Matlab/Simulink. Two different battery technologies are used to demonstrate the adaptability of this charger. The chosen simulation values are the ones available for getting experimental results and are presented in TABLE 1. Results are obtained using both a sinusoidal grid voltage and a grid voltage with harmonic distortion. Both conditions are analyzed in two different modes: G2V and V2G.

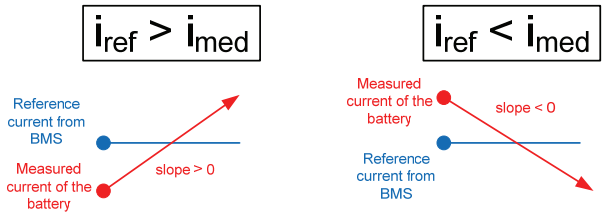

Fig.8. Hysteresis-Band to follow the reference current in the DC/DC converter

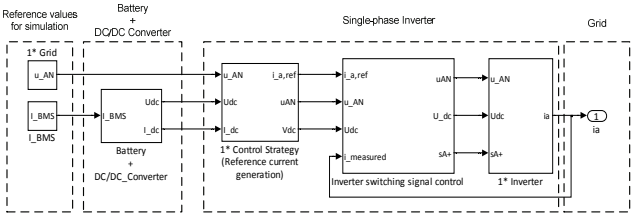

Fig.9. Non-linear battery model

Table 1. Parameters of the model

Battery	VHT F – Saft (10 batteries) -- (NiMH) MP 176065 Integration (4 batteries) -- (Li-ion)
RMS grid voltage	20 V
Grid frecuency	50 Hz
Bus voltage (U_{dc})	90 V
L_{DC}	10,540 mH
R_{DC}	0,153 Ω
L_{AC1}	15,848 mH
R_{AC1}	0,383 Ω
L_{AC2}	14,955 mH
R_{AC2}	0,383 Ω
Battery current	-3 A (G2V); 3 A (V2G)

Fig.10a and Fig.10b present the charger behaviour in the G2V and V2G modes, respectively, using a Li-ion battery and connected to an ideal grid voltage. The upper subplots show the phase-neutral grid voltage and the lower ones display the generated reference current and the demanded one (or the injected current, in case of V2G) to the grid. It can be checked that a sinusoidal current and against phase with the fundamental grid voltage is demanded if a G2V mode is being carried out (in phase with the fundamental grid voltage in case of a V2G mode). The THD_is (Total Harmonic Distortion of the grid current) are 4,2% and 4,0% for G2V and V2G modes, respectively.

The same specifications are simulated and displayed in Fig.11a and Fig11.b, but using a NiMH battery, and similar conclusions can be obtained. The THD_is are 4,9% and 4,5% for G2V and V2G modes, respectively.

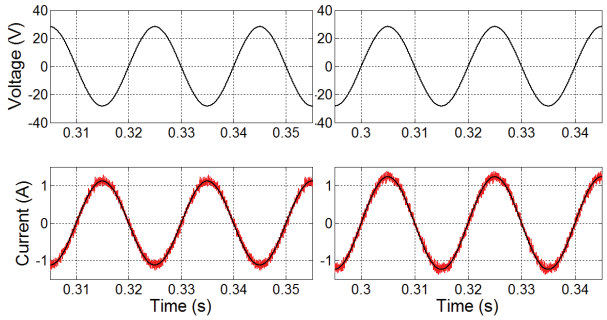

Fig.10. Ideal grid voltage. Li-ion battery. The upper subplots show the grid voltage and the lower ones the reference and real grid current for a) G2V and b) V2G modes.

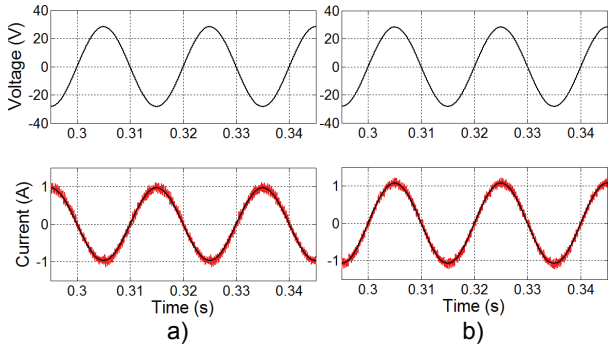

Fig.11. Ideal grid voltage. NiMH battery. The upper subplots show the grid voltage and the lower ones the reference and real grid current for a) G2V and b) V2G modes.

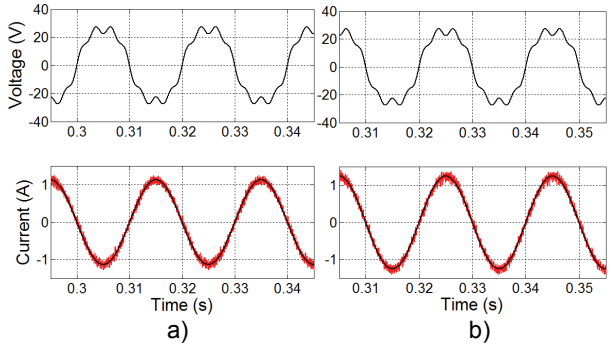

Fig.12. Distorted grid voltage (THD_{v3}=10% and THD_{v7}=10%). Li-ion battery. The upper subplots show the grid voltage and the lower ones the reference and real grid current for a) G2V and b) V2G modes.

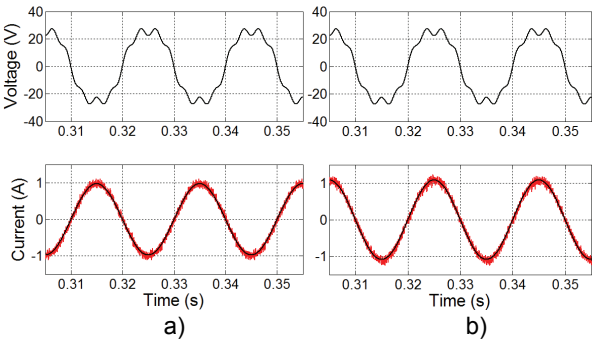

Fig.13. Distorted grid voltage (THD_{v3}=10% and THD_{v7}=10%). NiMH battery. The upper subplots show the grid voltage and the lower ones the reference and real grid current for a) G2V and b) V2G modes.

Starting from the conditions established to obtain Fig.10, the grid voltage is modified and a harmonic distortion is added: THD_{v3} = 10% and THD_{v7} = 10%. Fig.12 shows the same parameters displayed in Fig.10, taking into account the new grid voltage specifications. No distortion affect the reference current generation and therefore, a sinusoidal current is demanded (or injected) to the grid as in Fig.10. The new THD_is are 4,2% and 4,7% for G2V and V2G modes, respectively.

Fig.13 is obtained simulating the Fig.12 conditions, but using the NiMH battery. The battery type does not influence the operation of the bidirectional charger and no grid voltage distortion affect the reference current generation as occurred in Fig.12. The THD_is are 4,7% and 4,4% for G2V and V2G modes, respectively.

Experimental results

Once simulation results validated the battery charger topology, the control algorithms and the tracking technique, a prototype was built to corroborate the obtained results. The same specifications mentioned in Table 1 for simulation are used in the prototype to get the experimental measurements, which let us to compare the simulated results with the experimental ones. The control platform, DS1104 dSPACE, and three legs of a four legs SEMIKRON inverter, one of the legs for the DC/DC converter and two for the AC/DC converter (see Fig.1), are utilized to build the mentioned system. Tektronix TD5 510A oscilloscope is used to measure the desired signals.

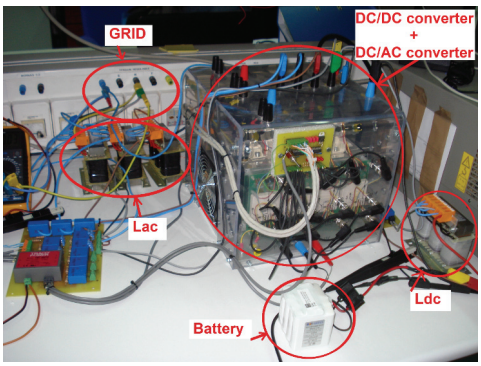

Fig.14. Prototype connected to an ideal voltage source.

Fig.14 and Fig.15 show the built prototype using a Li-ion battery and connected to an ideal voltage source and a distorted grid voltage, respectively.

Fig.16-Fig.21 show the grid voltage and current, according to the different conditions of the grid voltage, the different working modes (V2G and G2V) and the different battery types studied.

These figures correspond to Fig.10.a, Fig.10.b, Fig.11.a, Fig.11.b, Fig.12.a, Fig.12.b, Fig.13.a and Fig.13.b, respectively, which let us to compare the simulation and the experimental results and confirm all the ideas and theory developed above. Experimental figures also show the battery voltage and current to present the context in which the measurements were taken.

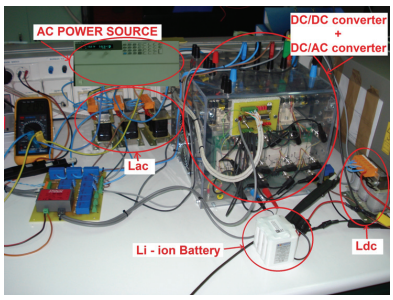

Fig.15. Prototype connected to a distorted grid voltage.

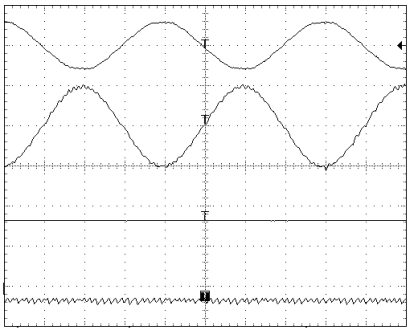

Fig.16. Ideal grid voltage. Li-ion battery. From top to bottom, grid voltage (50 V/div) and current (1 A/div) and battery voltage (25 V/div) and current (10 A/div). G2V mode.

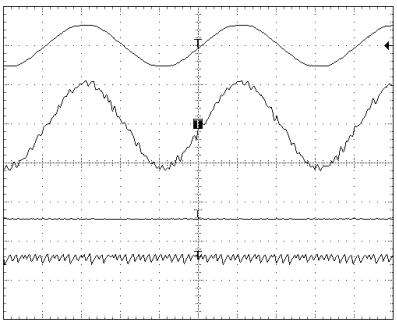

Fig.17. Ideal grid voltage. Li-ion battery. From top to bottom, grid voltage (50 V/div) and current (1 A/div) and battery voltage (25 V/div) and current (5 A/div). V2G mode.

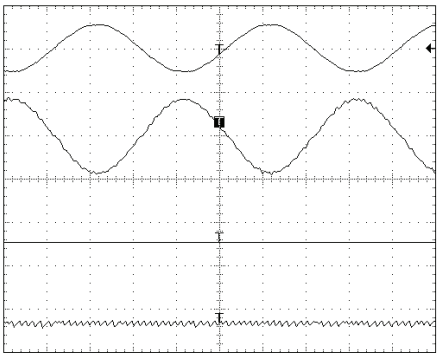

Fig.18. Ideal grid voltage. NiMH battery. From top to bottom, grid voltage (50 V/div) and current (1 A/div) and battery voltage (25 V/div) and current (10 A/div). G2V mode.

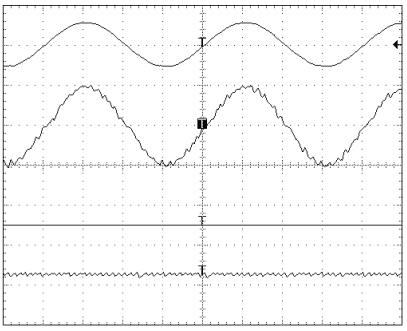

Fig.19. Ideal grid voltage. NiMH battery. From top to bottom, grid voltage (50 V/div) and current (1 A/div) and battery voltage (25 V/div) and current (10 A/div). V2G mode.

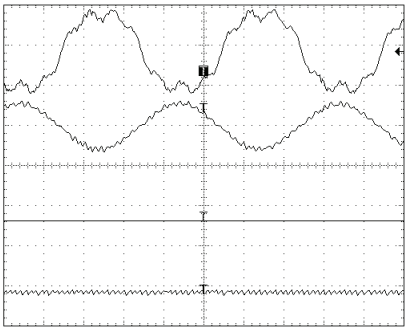

Fig.20. Distorted grid voltage (THD_{v3}=10% and THD_{v7}=10%). Li-ion battery. From top to bottom, grid voltage (30 V/div) and current (2 A/div) and battery voltage (25 V/div) and current (20 A/div). G2V mode.

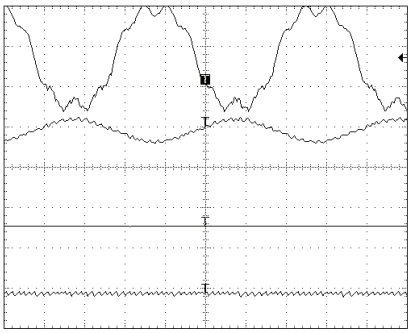

Fig.21. Distorted grid voltage (THD_{v3}=10% and THD_{v7}=10%). NiMH battery. From top to bottom, grid voltage (30 V/div) and current (5 A/div) and battery voltage (25 V/div) and current (20 A/div). G2V mode.

Conclusions

A new algorithm for a bidirectional charger for electric vehicle batteries has been proposed. A generic battery model has been implemented, which has been improved since the self-discharge effect has been included. The battery charger is implemented using a DC/DC converter together with an inverter. The novel control strategy proposed for this charger let the battery (any battery technology is allowed provided that all of its parameters values are within an admissible range) be charged (G2V) or discharged (V2G) demanding or injecting current into the grid with high quality: it is sinusoidal and with a unity displacement power factor, leading to the improvement of the power quality of the electric distribution system. This fact is the main contribution of this paper.

This bidirectional charger model has been validated since it has been subjected to different tests of simulation under ideal and distorted grid voltage, which in turn have

also been corroborated by experimental results, obtained with a built prototype configured using the same values of the simulation model.

This work was supported by the Spanish Ministry of Science and Innovation under the research project PSE-370000-2009-22, co-financed by FEDER. It was also supported by "Comunidad Autónoma de Extremadura" and co-financed by FSE.

REFERENCES

[1] S. Jaganathan, W. Gao, "Battery Charging Power Electronics Converter and Control for Plug-in Hybrid Electric Vehicle", *IEEE Conference Vehicle Power and propulsion*, (2009), pp. 440–447.

[2] M. Kisacikoblu, B. Ozpineci, L. Tolbert, "Examination of a PHEV Bidirectional Charger System for V2G Reactive Power Compensation", *IEEE Applied Power Electronics Conference and Exposition*, (2010), pp. 458–465.

[3] Lixin Tang, Gui-Jia Su, "A Low-Cost, Digitally-Controlled Charger for Plug-In Hybrid Electric Vehicles", *IEEE Energy Conversion Congress and Exposition*, (2009), pp. 3923–3929.

[4] I. Cvetkovic, T. Thacker, Dong Dong, G. Francis, V. Podosinov, D. Boroyevich, F. Wang, R. Burgos, G. Skutt, J. Lesko, "Future Home Uninterruptible Renewable Energy System with Vehicle-to-Grid Technology", *IEEE Energy Conversion and Exposition*, (2009), pp. 2675–2681.

[5] X. Zhou, S. Lukic, S. Bhattacharya, A. Huang, "Design and Control of Grid-connected Converter in Bi-directional Battery Charger for Plug-in Hybrid Electric Vehicle Application", *IEEE Vehicle Power and Propulsion Conference*, (2009), pp. 1716–1721.

[6] X. Zhou, G. Wang, S. Lukic, S. Bhattacharya, Huang, A., "Multi-Function Bi-directional Battery Charger for Plug-in Hybrid Electric Vehicle Application", *IEEE Energy Conversion Congress and Exposition*, (2009), pp. 3930–3936.

[7] Y.-J. Lee, A. Khaligh, A. Emadi, "Advanced Integrated Bidirectional AC/DC and DC/DC Converter for Plug-In Hybrid Electric Vehicles", *IEEE Journals Vehicular Technology*, vol. 58 (2009), pp. 3970–3980.

[8] B. Bilgin, E. Dal Santo, M. Krishnamurthy, "Universal Input Battery Charger Circuit for PHEV Applications with Simplified Controller", *IEEE Applied Power Electronics Conference and Exposition (APEC)*, (2011), pp. 815-820.

[9] M. Ortúzar et. al., "Implementation and Evaluation of an Ultracapacitor-Based Auxiliary Energy System for Electric Vehicles", *IEEE Transactions on Industrial Electronics*, vol. 54 (2007), issue 4, pp. 2147-2156.

[10] J. Zhang, S. Ci, H. Sharif, M. Alahmad, "An Enhanced Circuit-Based Model for Single-Cell Battery". *Power Electronics Conference and Exposition (APEC) 2010 Twenty-fifth Annual IEEE*, (2010), pp. 672–675.

[11] M. Zheng, B. Qi, X. Du, "Dynamic Model for Characteristics of Li-Ion Battery on electric Vehicle", *4th IEEE Conference Industrial Electronics and Applications*, (2009), pp. 2867–2871.

[12] R. Kroeze, P. Krein, "Electrical Battery Model for Use in Dynamic Electric Vehicle Simulations", *IEEE Conference Power Electronics Specialists*, (2008), pp. 1336-1342.

[13] M. Einhorn, V.F. Conte, C. Kral, J. Fleig, R. Permann, "Parameterization of an Electrical Battery Model for Dynamic System Simulation in Electric Vehicles", *IEEE Vehicle Power and Propulsion Conference (VPPC)*, (2010), p. 1.

[14] Xue-Zhe Wei, XiaoPeng Zhao, YongJun Yuan, "Study of Equivalent Circuit Model for Lead-Acid Batteries in Electric Vehicle", *IEEE Measuring Technology and mechatronics Automation*, vol. 2 (2009), pp.685-690.

[15] C. Sen, N. C. Kar, "Battery Pack Modeling for the Analysis of the Battery Management System of a Hybrid Electric Vehicle", *IEEE Vehicle Power and Propulsion Conference*, (2009), p. 207.

[16] O. Tremblay, L.-A. Dessaint, A.-I. Dekkiche, "A Generic Battery Model for the Dynamic Simulation of Hybrid Electric Vehicles", *IEEE Conference Vehicle Power and Propulsion*, (2008), pp. 284–289.

[17] M. Milanés-Montero et. Al., "Novel Method for Synchronization to Disturbed Three-Phase and Single-Phase Systems", *IEEE International Symposium on Industrial Electronics*, (2004).

***Authors**: eng. Javier Gallardo-Lozano, jagallardo@peandes.unex.es; dr eng. María Isabel Milanés-Montero, milanes@unex.es; eng. Miguel Ángel Guerrero-Martinez, mguerrero@peandes.unex.es; dr eng. Enrique Romero-Cadaval, eromero@unex.es. University of Extremadura, School of Industrial Engineering, Avda. Elvas s/n 06006 Badajoz.*